Available online at www.sciencedirect.com
SCIENCE DIRECT®
Journal of Computational Physics 202 (2005) 216–235
JOURNAL OF COMPUTATIONAL PHYSICS
www.elsevier.com/locate/jcp

Accurate numerical methods for the collisional motion of (heated) granular flows

Francis Filbet [a], Lorenzo Pareschi [b,*], Giuseppe Toscani [c]

[a] *Mathématiques et Applications, Physique Mathématique d'Orléans (MAPMO), CNRS – Université d'Orléans, B.P. 6759, 45067 Orléans, France*
[b] *Dipartimento di Matematica, Universitá di Ferrara, Via Machiavelli 35, 44100 Ferrara, Italy*
[c] *Dipartimento di Matematica, Universitá di Pavia, Via Ferrata 1, 27100 Pavia, Italy*

Received 10 March 2004; received in revised form 18 June 2004; accepted 18 June 2004
Available online 9 September 2004

Abstract

In this paper, we extend the spectral method developed in [L. Pareschi, B. Perthame, A Fourier spectral method for homogeneous Boltzmann equations, Trans. Theo. Stat. Phys. 25 (1996) 369–383; L. Pareschi, G. Russo, Numerical solution of the Boltzmann equation I: Spectrally accurate approximation of the collision operator, SIAM J. Numer. Anal. 37 (2000) 1217–1245] to the case of the inelastic Boltzmann equation describing the collisional motion of a granular gas with and without a heating source. The schemes are based on a Fourier representation of the equation in the velocity space and provide a very accurate description of the time evolution of the distribution function. Several numerical results in dimension one to three show the efficiency and accuracy of the proposed algorithms. Some mathematical and physical conjectures are also addressed with the aid of the numerical simulations.

AMS: 65L60; 65R20; 76P05; 82C40
Keywords: Inelastic Boltzmann equation; Spectral methods; Granular gases; Homogeneous cooling

1. Introduction

In kinetic theory, granular fluids far from equilibrium are usually modelled by inelastic hard spheres describing dissipative short range interactions between molecules. The interest in granular matter has strongly stimulated new developments in kinetic theory of granular gases.

* Corresponding author.
E-mail addresses: filbet@labomath.univ-orleans.fr (F. Filbet), pareschi@dm.unife.it, prl@dns.unife.it (L. Pareschi), toscani@dimat.unipv.it (G. Toscani).

0021-9991/$ - see front matter
doi:10.1016/j.jcp.2004.06.023

A granular gas can be viewed as a set of large macro-particles with short range repulsive core interactions, in which energy is lost in the inelastic collisions. These macro-particles are described by a distribution function $f(t, x, v)$, which depends on time $t \geqslant 0$, position $x \in \mathbb{R}^d$ and velocity $v \in \mathbb{R}^d$, $d \geqslant 1$, and solves a Boltzmann type equation [15–17]

$$\frac{\partial f}{\partial t} + v \cdot \nabla_x f = Q(f, f). \tag{1}$$

The collision operator $Q(f, f)$ describes the binary collisions, which only conserve mass and momentum since energy is dissipating. The inelastic collisions are characterized by a restitution coefficient e $(0 < e < 1)$, where $(1 - e^2)$ measures the degree of inelasticity.

Granular gases reveal a rich variety of self-organized structures such as large scale clusters, vertex fields, characteristic shock waves and others, which are still far from being completely understood. Applications of such systems range from astrophysics (stellar clouds, planetary rings), to industrial processes (handling of pharmaceuticals) and environment (pollution, erosion processes). Despite their importance in applications, deterministic numerical studies involving the full three-dimensional Boltzmann or Enskog dissipative kinetic equations have never been addressed before.

As a first step towards the numerical solution to the full problem, in this paper we will focus on the time evolution and the steady states of self-similar solutions to (1) in the spatially homogeneous case. There are several reasons behind this choice. First of all, the numerical study of the homogeneous cooling process is of major importance to understand the physics of such systems and for the construction of suitable equations of hydrodynamics. Non-Maxwellian equilibrium states, finite time energy extinction and quasi-elastic asymptotics [36,28,4] are just some of the non-trivial homogeneous behaviors. Not to mention the fact that most of the numerical difficulties related to the solution of (1) are due to the presence of $Q(f, f)$ and not to the transport part or the additional heating source.

Second, from a theoretical point of view, the study of the large-time behavior of the solution to the spatially homogeneous Boltzmann equation received a lot of interest in recent years, and essential progresses have been made in particular on the Boltzmann equation for inelastic Maxwell particles, both for the free case without energy input [4,10], and for the driven case [13,14,5].

It is remarkable that, on the contrary to elastic collisions, partially inelastic collisions have a non-trivial outcome as well in one dimension, and the one-dimensional idealization is a non-trivial adjunct to more realistic studies. One-dimensional Maxwellian inelastic gases where studied in [1]. This study led to the discovery of an exact similarity solution for a freely cooling Maxwellian inelastic gas [1] (which corresponds to the well known "BKW" solution [3,18] since they are identical in the Fourier space as explained in [5]). This solution, which has an algebraic high energy tail like $1/v^4$, can be used to test the class of initial values that are attracted in large-time. A different one-dimensional kinetic equation, which can be considered as a dissipative version of Kac's model, have been recently introduced in [32] to fully understand, at least in simplified models, the importance of the amount of dissipation in the cooling problem.

Real models, in which particles undergo binary hard-sphere interactions, or the coefficient of restitution depends on the relative velocity, have been less studied. The behavior of a hard-sphere granular gas in presence of some additional external source of energy in the system (a heat operator), has been recently investigated in [24], and the existence of non-trivial stationary states has been found.

Here, we will extend the spectral method recently presented in [30,31] for the classical Boltzmann equation to the inelastic situation. At variance to Monte Carlo methods the spectral method has shown to be extremely accurate and thus very suitable to test mathematical and physical conjectures. We refer the reader to [17,29,22] for a detailed discussion on spectral methods for the Boltzmann equation and their application to non-homogeneous situations. Finally, we mention here some recent works where the numerical solution of some kinetic model for granular gases has been considered [28,25].

The rest of the paper is organized as follows. In Section 2, we give a brief overview of the inelastic Boltzmann equation and the properties of its solution. In Section 3, we describe the spectral method for the heated inelastic Boltzmann model. In Sections 4 and 5, we present different numerical results in one dimension to check the accuracy of the method and the study of the stationary states. A particular care has been devoted to the accurate the treatment of the large time behaviors. Finally numerical simulations are performed in the whole 3D velocity space. Our analysis will take essential advantages from the knowledge of various theoretical results concerned with Maxwellian models. Among others properties, the inelastic Maxwell models exhibit similarity solutions, and these solutions represent the intermediate asymptotic of a wide class of initial conditions. In particular, Ernst and Brito [19,20,27,2,9] conjectured that these self-similar solutions must have a typical tail property. The first proof of Ernst–Brito conjecture for a sub-class of isotropic initial conditions was obtained in [6]. The restriction to the initial condition was subsequently removed in [7], where it was proven that the self-similar solution attracts all data which initially have finite moments of some order greater than two.

2. The governing equation

In absence of external forces the time evolution of a granular gas can be described at the kinetic level by the inelastic Boltzmann equation (1). Note that, in contrast with the elastic case, the one-dimensional $d = 1$ inelastic Boltzmann equation can be considered (see [35,28]). For the sake of generality, in the sequel we will refer to the multidimensional case $d \geqslant 2$. The reduction to the one-dimensional case is straightforward and will be omitted.

As already mentioned in Section 1, we will restrict here to the (heated) space homogeneous case

$$\frac{\partial f}{\partial t} - \epsilon \Delta_v f = Q(f, f), \tag{2}$$

where $\epsilon \geqslant 0$ is a small diffusion coefficient.

Let v and v_* be the velocities of the two particles before a collision, and denote by $g = v - v_*$ their relative velocity. Let the primes denote the same quantities after the collision. Then, the post-collisional velocities are found by assuming the total conservation of mass and momentum, and a partial loss of the normal relative velocity

$$n \cdot g' = -e(g \cdot n), \tag{3}$$

where n is the unit vector in the direction of impact, and $0 < e < 1$ is the coefficient of normal restitution, which in general depends on the relative velocity before collision $e \equiv e(|v - v_*|)$. By using this, we can construct the post-collisional velocities as follows

$$v' = \frac{v + v_*}{2} + \frac{1 - e}{4}(v - v_*) + \frac{1 + e}{4}|v - v_*|n, \tag{4}$$

$$v'_* = \frac{v + v_*}{2} - \frac{1 - e}{4}(v - v_*) - \frac{1 + e}{4}|v - v_*|n. \tag{5}$$

In the literature, essentially for simplicity reasons, it is frequently assumed that the restitution coefficient is a physical constant. In real systems, the situation is in general rather intricate [33]. In general, the restitution coefficient may depend on the relative velocity in such a way that collisions with small relative velocity are close to be elastic. The simplest physically correct description of dissipative collisions is based on the assumption that the spheres are composed by viscoelastic material, which is in good agreement with experimental data. In this case, the velocity-dependent restitution coefficient for viscoelastic spheres of diameter $\sigma > 0$ and mass m reads [11]

$$e = 1 - C_1 A \alpha^{2/5} |v - v_*|^{1/5} + C_2 A^2 \alpha^{4/5} |v - v_*|^{2/5} \pm \cdots, \tag{6}$$

with

$$\alpha = \frac{3\sqrt{3}}{2} \frac{\sqrt{\sigma} Y}{m(1 - \nu^2)}, \tag{7}$$

where Y is the Young modulus, ν is the Poisson ratio, and A depends on dissipative parameters of the material. The constant C_1 and C_2 can be explicitly computed.

Let us note that for a constant restitution coefficient, inverse relations of (4) and (5) can be explicitly computed, tracing collision history back from the pair v, v_* to their predecessors, which we denote by ${}'v$ and ${}'v_*$

$${}'v = \frac{v + v_*}{2} - \frac{1 - e}{4e}(v - v_*) + \frac{1 + e}{4e}|v - v_*| n, \tag{8}$$

$${}'v_* = \frac{v + v_*}{2} + \frac{1 - e}{4e}(v - v_*) - \frac{1 + e}{4e}|v - v_*| n. \tag{9}$$

We stress here the fact that we cannot identify, as it is commonly done in the elastic case, pre-collisional and post-collisional velocities since the Jacobian of the transformation is different from one.

Now, let us define the collision operator in (2) by its action on test functions. Taking $\psi \equiv \psi(t, v)$ to be a suitably regular test function, we set

$$\int Q(f, f)(v)\psi = \frac{1}{2} \int_{\mathbb{R}^d} \int_{\mathbb{R}^d} \int_{S^{d-1}} B(g, n) f f_* (\psi' + \psi'_* - \psi - \psi_*) \mathrm{d}n \, \mathrm{d}v \, \mathrm{d}v_*. \tag{10}$$

Here and below we use the shorthand notations $f = f(t, v)$, $f_* = f(t, v_*)$, and so on. The function $B(g, n)$ is taken as the variable hard sphere interaction kernel

$$B(g, n) = C_\lambda |g|^\lambda. \tag{11}$$

The case $\lambda = 0$ stands for the Maxwellian molecules, which has been widely studied because it strongly simplifies the mathematical analysis. However the only physical model that seems reasonable for granular gases is the hard-sphere model, which corresponds to $\lambda = 1$. Other models are also obtained for $0 < \lambda < 1$.

Using the weak form (10) allows us to study equations for average values of observable given by the functionals of the form $\int_{\mathbb{R}^d} f\psi \, \mathrm{d}v$. Now, in the case $\epsilon = 0$, multiplying Eq. (2) by a test function ψ we obtain

$$\frac{\mathrm{d}}{\mathrm{d}t} \int_{\mathbb{R}^d} f\psi \, \mathrm{d}v = \int_{\mathbb{R}^d} Q(f, f)\psi \, \mathrm{d}v, \tag{12}$$

with the weak form (10) of the collision operator, it is easy to check at least formally the basic conservation relations that follows from (2). Namely, setting $\psi \equiv 1$ and $\psi \equiv v$ in (10), we obtain the conservation of mass and momentum

$$\int_{\mathbb{R}^3} Q(f, f) \begin{pmatrix} 1 \\ v \end{pmatrix} \mathrm{d}v = 0. \tag{13}$$

Furthermore, taking $\psi = |v|^2$ and computing

$$|v'|^2 + |v'_*|^2 - |v|^2 - |v_*|^2 = -\frac{1 - e^2}{2} \frac{|g| - (g \cdot n)}{2} |g|,$$

we obtain the following relation for the dissipation of the kinetic energy

$$\frac{\mathrm{d}}{\mathrm{d}t}\int_{\mathbb{R}^d} f|v|^2\,\mathrm{d}v = -C_\lambda\frac{1-e^2}{8}\int_{\mathbb{R}^d\times\mathbb{R}^d}\left(\int_{S^{d-1}}(|g|-g\cdot\omega)d\omega\right)|g|^{\lambda+1}ff_*\,\mathrm{d}v\,\mathrm{d}v_* \leqslant 0. \tag{14}$$

Finally, any function f for which $Q(f,f)=0$ has the form of a locally Dirac-distribution

$$\delta_{\rho,u}(v) = \rho\delta(|v-u|), \tag{15}$$

where ρ, u are the density and mean velocity of the gas

$$\rho = \int_{\mathbb{R}^d} f(v)\mathrm{d}v, \quad u = \frac{1}{\rho}\int_{\mathbb{R}^d} vf(v)\mathrm{d}v. \tag{16}$$

The temperature is given by

$$T = \frac{1}{d}\left(\frac{1}{\rho}\int_{\mathbb{R}^d}|u-v|^2 f(v)\mathrm{d}v\right), \tag{17}$$

and goes to zero when time goes to infinity.

Let us consider an initial datum such that

$$\rho = 1, \quad u = 0.$$

In the Maxwellian case the relaxation of the temperature ($C_0 = 1/2\pi$) is explicitly given by

$$T(t) = T(0)\exp\left(-\frac{(1-e^2)}{2}t\right). \tag{18}$$

In general, if $\lambda > 0$ (variable hard sphere), the equation for the temperature is not closed, and the kinetic temperature is shown only to satisfy inequalities [24]

$$\frac{\mathrm{d}T}{\mathrm{d}t} \leqslant -C_\lambda\pi\frac{(1-e^2)}{4}T^{(2+\lambda)/2}. \tag{19}$$

Using the weak form (10), we can also derive the strong form of the collision operator. We notice the obvious splitting into "gain" and "loss" terms

$$Q(f,f) = Q^+(f,f) - Q^-(f,f).$$

Assuming that f is smooth enough, setting $\psi = \delta(v - v_0)$ in the part of (10) corresponding to $Q^-(f,f)$, we find

$$Q^-(f,f) = C_\lambda\int_{\mathbb{R}^d}\int_{S^{d-1}} ff_*|v-v_*|^\lambda\,\mathrm{d}n\,\mathrm{d}v_*.$$

To find the explicit form of $Q^+(f,f)$ we need to invoke the inverse collision transformation, tracing collision history back from the pair v, v_* to their predecessors, which we denote by $'v$ and $'v_*$. Setting $\psi(v) = \delta(v - v_0)$ we obtain

$$Q^+(f,f) = C_\lambda\int_{\mathbb{R}^d}\int'_{S^{d-1}} f'f_*J|v-v_*|^\lambda\,\mathrm{d}n\,\mathrm{d}v_*, \tag{20}$$

where $'f = f(t,'v)$, $'f_* = f(t,'v_*)$, and J is related to the Jacobian of the transformation from post-collisional to pre-collisional velocities, $(v, v_*) \to ('v, 'v_*)$. In the general case, we only know the inverse transformation given by (4) and (5) and for constant restitution coefficient e, it is given by (8) and (9) and

$$J = \frac{1}{e^2}\frac{|'v-'v_*|^\lambda}{|v-v_*|^\lambda}.$$

3. Spectral approximation of the collision operator

From now let us concentrate to the most interesting case: hard sphere molecules

$$B(g,n) = C_1|g|.$$

However a similar analysis can be performed for Maxwellian molecules and more general model (11).

As extensively discussed in [31] the first step in the derivation of a spectral method is to describe the action of the collision operator with respect to compactly supported density function f.

To this aim we consider the space homogeneous Boltzmann equation (2) without diffusion in the weak form (10), which can be written for any smooth test function ψ

$$\int Q(f,f)(v)\psi(v)\mathrm{d}v = \frac{C_1}{2}\int_{\mathbb{R}^d}\int_{\mathbb{R}^d}\int_{S^{d-1}}|g|f(v)f(v-g)(\psi(v')-\psi(v))\mathrm{d}n\,\mathrm{d}g\,\mathrm{d}v,$$

where $g = v - v_*$, and

$$v' = v - \frac{1+e}{4}(g-|g|n).$$

The extension of the spectral method to the uniformly heated case ($\epsilon > 0$) is straightforward and will be omitted.

Lemma 3.1. *Let* $\mathrm{supp}(f(v)) \subset \mathscr{B}(0,R)$ *where* $\mathscr{B}(0,R)$ *is the ball of radius R centered in the origin. Then we have*

(*i*) $\mathrm{Supp}(Q(f,f)(v)) \subset \mathscr{B}(0,\sqrt{2}R)$,

(*ii*) $$\int Q(f,f)(v)\psi(v)\mathrm{d}v = \frac{C_1}{2}\int_{\mathscr{B}(0,\sqrt{2}R)}\int_{\mathscr{B}(0,2R)}\int_{S^{d-1}}|g|f(v)f(v-g)(\psi(v')-\psi(v))\mathrm{d}n\,\mathrm{d}g\,\mathrm{d}v,$$

with $v-g \in \mathscr{B}(0,(2+\sqrt{2})R)$ *and* $v' \in \mathscr{B}(0,(1+e+\sqrt{2})R)$.

Proof. First we prove (i). If ${}'v, {}'v_* \in \mathscr{B}(0,R)$, then

$$|v|^2 \leqslant |v|^2 + |v_*|^2 \leqslant (|{}'v|)^2 + (|{}'v_*|)^2 \leqslant 2R^2$$

and also

$$|g| = |v - v_*| \leqslant |{}'v - {}'v_*| \leqslant 2R.$$

If ${}'v$ (or ${}'v_*$) $\notin \mathscr{B}(0,R)$, then

$$f({}'v) = 0 \text{ (or } f({}'v_*) = 0),$$

and the identity is clear.

Next we prove (ii). If $v \in \mathscr{B}(0,\sqrt{2}R)$ and $g \in \mathscr{B}(0,2R)$ we have

$$|v-g| \leqslant |v| + |g| \leqslant (\sqrt{2}+2)R,$$

and

$$|v'| \leqslant |v| + \frac{1+e}{2}|g| \leqslant (\sqrt{2}+(1+e))R. \qquad \square$$

Remark 3.1. Note that for the elastic case there is no difference if we use the strong or the weak form of the operator in deriving the above proposition. This is due to the fact that we can identify pre and post collisional particles in the elastic case. This is no more valid in the inelastic case. However in both cases, elastic and inelastic, the correct derivation of the bound is in weak form, since the spectral method is based on the weak form of the equation.

As a consequence, as in the elastic case [31], in order to write a spectral approximation to (2) for a compactly supported distribution function $f(v)$ we can consider $f(v)$ restricted on $[-V, V]^d$ with $V \geqslant (3+\sqrt{2})R/2 = R/\lambda$, assuming $f(v) = 0$ on $[-V, V]^d \setminus \mathscr{B}(0, R)$, and extend it by periodicity to a periodic function on $[-V, V]^d$. As shown in [28] in the one-dimensional case the resulting inelastic collision operator has compact support in $[-R, R]$. Thus the solution remains compactly supported for all later times. In this simpler case it is enough to take $V \geqslant 2R$ to avoid aliasing errors.

In general, if the distribution function is well approximated by a function with compact support in velocity space, then the above approximation will provide an accurate evaluation of the collision integral.

To simplify the notation let us take $V = \pi$. Hereafter, we used just one index to denote the d-dimensional sums with respect to the vector $k = (k_1, \ldots, k_d) \in \mathbb{Z}^d$, hence we set

$$\sum_{k=-N}^{N} = \sum_{k_1,\ldots,k_d=-N}^{N}.$$

The approximate function f_N is represented as the truncated Fourier series

$$f_N(v) = \sum_{k=-N}^{N} \hat{f}_k \, \mathrm{e}^{\mathrm{i}k\cdot v}, \tag{21}$$

$$\hat{f}_k = \frac{1}{(2\pi)^d} \int_{[-\pi,\pi]^d} f(v) \mathrm{e}^{-\mathrm{i}k\cdot v} \, \mathrm{d}v.$$

In a Fourier–Galerkin method the fundamental unknowns are the coefficients $\hat{f}_k, k = -N, \ldots, N$. We obtain a set of ODEs for the coefficients $\hat{f}_k$ by requiring that the residual of (2) be orthogonal to all trigonometric polynomials of degree $\leqslant N$. Hence for $k = -N, \ldots, N$

$$\int_{[-\pi,\pi]^d} \left(\frac{\partial f_N(v)}{\partial t} - Q(f_N, f_N)(v) \right) \mathrm{e}^{-\mathrm{i}k\cdot v} \, \mathrm{d}v = 0,$$

with

$$\int_{[-\pi,\pi]^d} Q(f_N, f_N)(v) \mathrm{e}^{-\mathrm{i}k\cdot v} \, \mathrm{d}v = \frac{C_1}{2} \int_{[-\pi,\pi]^d} \int_{\mathscr{B}(0,2\lambda\pi)} \int_{S^{d-1}} |g| f_N(v) f_N(v-g) \left(\mathrm{e}^{-\mathrm{i}k\cdot v'} - \mathrm{e}^{-\mathrm{i}k\cdot v} \right) \mathrm{d}n \, \mathrm{d}g \, \mathrm{d}v.$$

Using expression (21) we get the set of ODEs

$$\frac{\partial \hat{f}_k}{\partial t} = \sum_{\substack{l,m \\ l+m=k}}^{N} \hat{f}_l \hat{f}_m (\hat{B}(l,m) - \hat{B}(m,m)), \tag{22}$$

where the *kernel modes* $\hat{B}(l, m)$ are given by

$$\hat{B}(l,m) = \frac{C_1}{2} \int_{\mathscr{B}(0,2\lambda\pi)} \int_{S^{d-1}} |g| \mathrm{e}^{-\mathrm{i}mg + \mathrm{i}(l+m)(1+e)(g-|g|n)/4} \, \mathrm{d}n \, \mathrm{d}g. \tag{23}$$

The evaluation of the right hand side of (22) requires exactly $\mathscr{O}(N^{2d})$ operations. We emphasize that the usual cost for a method based on N^d parameters for f in the velocity space is $\mathscr{O}(N^{2d}M)$ where M is the numbers of angle discretizations. The loss term on the right hand side is a convolution sum and thus transform methods allow this term to be evaluated only in $\mathscr{O}(N^d \log N)$ operations. Hence the most expensive part of the computation is represented by the gain term.

3.1. Analysis of the kernel modes

In this section, we study the main characteristics of the kernel modes and in particular we give an explicit representation of them in the case of constant coefficient of restitution.

Let us start from Eq. (23). One has

$$\hat{B}(l,m) = \frac{C_1}{2}\int_{\mathscr{B}(0,2\lambda\pi)} |g| \exp\left(\mathrm{i}g\cdot l\frac{1+e}{4} - \mathrm{i}g\cdot m\frac{3-e}{4}\right)\mathscr{I}_0(|g|, l+m, e)\mathrm{d}g, \tag{24}$$

where

$$\mathscr{I}_0(|g|, l+m, e) = \int_{S^{d-1}} \exp\left(-\mathrm{i}|g| n\cdot(l+m)\frac{1+e}{4}\right)\mathrm{d}n. \tag{25}$$

Following the same computations as in [31] we have to distinguish between the 3D and 2D collision model.

3.2. 3D case

Let $q = |g|(l+m)(1+e)/4$. Then

$$\mathscr{I}_0(|g|, l+m, e) = \int_{S^2} \mathrm{e}^{-\mathrm{i}q\cdot n}\,\mathrm{d}n = 4\pi\,\mathrm{Sinc}(|q|) = 4\pi\,\mathrm{Sinc}\left(\frac{|g||l+m|(1+e)}{4}\right) \tag{26}$$

where

$$\mathrm{Sinc}(x) \equiv \frac{\sin x}{x}.$$

Let $p = l(1+e)/4 - m(3-e)/4$. Then, taking into account the previous result, one has

$$\hat{B}(l,m) = C_1 2\pi \int_{\mathscr{B}(0,2\lambda\pi)} |g|\,\mathrm{Sinc}(|g||l+m|(1+e)/4)\exp(\mathrm{i}p\cdot g)\mathrm{d}g.$$

Making use of spherical coordinates, with $\rho = |g|$, one has

$$\begin{aligned}\hat{B}(l,m) &= C_1 4\pi^2 \int_0^{2\pi\lambda} \rho^3\,\mathrm{Sinc}(|l+m|(1+e)\rho/4)\mathrm{d}\rho \int_0^{\pi} \exp(\mathrm{i}|p|\rho\cos\theta)\sin\theta\,\mathrm{d}\theta \\ &= C_1 8\pi^2 \int_0^{2\pi\lambda} \rho^3\,\mathrm{Sinc}(|l+m|(1+e)\rho/4)\,\mathrm{Sinc}(|l(1+e)-m(3-e)|\rho/4)\mathrm{d}\rho.\end{aligned}$$

With the change of variables $\rho = 2\lambda\pi r$ the coefficient $\hat{B}(l,m)$ can be written as

$$\hat{B}(l,m) = C_1 8\pi^2(2\lambda\pi)^4 \int_0^1 r^3\,\mathrm{Sinc}(\xi r)\,\mathrm{Sinc}(\eta r)\mathrm{d}r,$$

where $\xi = |l+m|(1+e)\lambda\pi/2$, $\eta = |l(1+e)-m(3-e)|\lambda\pi/2$. To simplify notations let us assume that

$$C_1 = (8\pi^2(2\lambda\pi)^4)^{-1}.$$

In this case the coefficient can be written as

$$\hat{B}(l,m) = F(\xi,\eta) = \int_0^1 r^3\,\mathrm{Sinc}(\xi r)\,\mathrm{Sinc}(\eta r)\mathrm{d}r. \tag{27}$$

It is easy to prove that for constant coefficient of restitution (27) has an explicit analytical expression given by

$$F(\xi,\eta) = \frac{((\xi-\eta)\sin(\xi-\eta)+\cos(\xi-\eta))}{2\xi\eta(\xi-\eta)^2} - \frac{((\xi+\eta)\sin(\xi+\eta)+\cos(\xi+\eta))}{2\xi\eta(\xi+\eta)^2} - \frac{2}{(\xi+\eta)^2(\xi-\eta)^2}. \tag{28}$$

For more general coefficient of restitution $e = e(|g|)$ the computation of the kernel modes requires only the evaluation of a one-dimensional integral that can be pre-computed and stored in a suitable array.

3.3. 2D case

For the computation in 2D we start from Eqs. (24) and (25).
In this case it is

$$\mathscr{I}_0 = \int_S \exp(-\mathrm{i}q\cdot n)\mathrm{d}n = 2\int_0^\pi \cos(|q|\cos\theta)\mathrm{d}\theta = 2\pi J_0(|q|) \tag{29}$$

where J_0 is the Bessel function of order 0. By inserting the result in the expression (24) for $\hat{B}(l,m)$, one has

$$\hat{B}(l,m) = C_1\pi\int_{\mathscr{B}(0,2\lambda\pi)} |g|\exp(\mathrm{i}g\cdot p)J_0(|l+m||g|(1+e)/4)\mathrm{d}g.$$

Making use of polar coordinates, the expression for the coefficients becomes

$$\begin{aligned}\hat{B}(l,m) &= C_1\pi\int_0^{2\pi\lambda}\rho^2\left(\int_0^{2\pi}\cos(|l(1+e)-m(3-e)|\rho/4)\cos\theta\,\mathrm{d}\theta\right)J_0(|l+m|(1+e)\rho/4)\mathrm{d}\rho\\ &= C_1 2\pi^2\int_0^{2\pi\lambda}\rho^2 J_0(|l(1+e)-m(3-e)|\rho/4)J_0(|l+m|(1+e)\rho/4)\mathrm{d}\rho\\ &= C_1 2\pi^2(2\pi\lambda)^3\int_0^1 r^2 J_0(\xi r)J_0(\eta r)\mathrm{d}r.\end{aligned} \tag{30}$$

Taking now $C_1 = (2\pi^2(2\pi\lambda)^3)^{-1}$, the expression of $\hat{B}(l,m)$ becomes

$$\hat{B}(l,m) = F(\xi,\eta) = \int_0^1 r^2 J_0(\xi r)J_0(\eta r)\mathrm{d}r. \tag{31}$$

Note that again in this case each kernel mode can be computed as a 1D integral and stored in an array.

4. Numerical applications

In this section, we test the spectral method for several physical problems when applied to different granular models. In particular we will make use of a suitable rescaling technique as in [23] to deal efficiently with the approximation of steady states of the inelastic Boltzmann equation. The choice of the computational domain in all the tests presented is done carefully in order to balance the errors due to aliasing and resolution (we refer to [31] for a detailed discussion on this topic).

4.1. 1D models for Maxwellian molecules

In this section, we investigate the case of Pseudo-Maxwellian molecules, which is interesting to test the accuracy of the methods since analytical results are available [6,7]. Indeed, introducing the Fourier representation for f,

$$\phi(t,k) = \int_{\mathbb{R}} f(t,v)\exp(-\mathrm{i}kv)\mathrm{d}v,$$

then, the equation for ϕ reads as follows [5]

$$\frac{\partial \phi}{\partial t} = \phi(zk)\phi((1-z)k) - \phi(0)\phi(k), \quad k \in \mathbb{R}.$$

4.1.1. Inelastic Boltzmann equation

We first consider the inelastic Boltzmann equation, where the solution formally converges to a Dirac delta equilibrium state. We perform this test to check the spectral accuracy of the method and the rescaling technique to approximate accurately the asymptotic behavior of the equation.

The accuracy of the method has been verified by direct comparison with the evolution of the temperature which is analytically given by (18).

In the following test cases we consider several initial data with the same mass, mean velocity and temperature, but with different shapes

$$\text{(i) } f_0(v) = \frac{1}{\sqrt{2\pi}}\exp(-|v|^2/2),$$

$$\text{(ii) } f_0(v) = \frac{1}{2\sigma\sqrt{2\pi}}\left(\exp\left(-\frac{|v-3\sigma|^2}{2\sigma^2}\right) + \exp\left(-\frac{|v+3\sigma|^2}{2\sigma^2}\right)\right), \quad \sigma^2 = 1/10,$$

$$\text{(iii) } f_0(v) = \frac{16}{5\sigma\pi(1+|v|^2/\sigma^2)^4}, \quad \sigma^2 = 5.$$

4.1.1.1. Classical variables. We consider initial data (i) and (ii) and perform computations with different number of Fourier modes $N = 8, 16, 32, 64$. The spectral convergence of the method for small times clearly appears from Fig. 1 where the relative L_1-error in logarithmic scale is reported. However for longer times since the solution converges towards a Dirac delta equilibrium states we observe spurious oscillations due to the Gibbs phenomenon [12,26] and thus we have a marked deterioration of accuracy (see also Fig. 4(a)).

There are two different strategies that may serve as a remedy to this problem. One possibility is to add a 'fictitious' diffusive source of energy that acts as a numerical viscosity in order to avoid the oscillations [28].

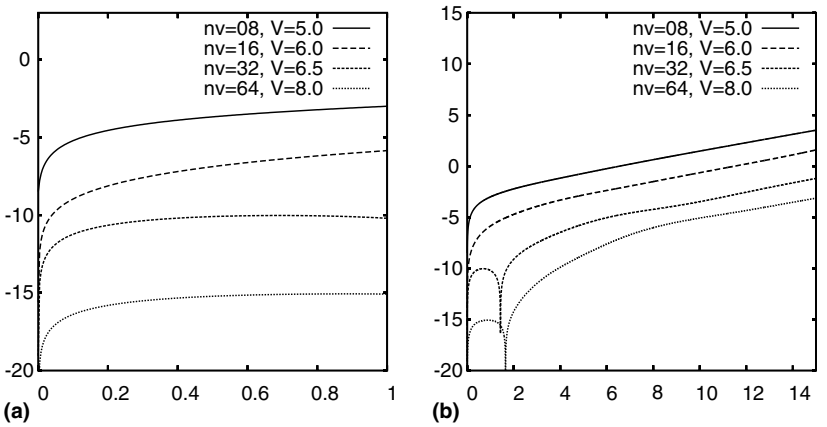

Fig. 1. 1D inelastic Maxwellian molecules: short and long time error for initial datum (i).

However the choice of the numerical viscosity is a delicate aspect. A more robust strategy consists in rescaling the equation in a suitable way as explained in the next paragraph.

4.1.1.2. Rescaled variables. As observed in the previous example, the relaxation of the temperature cannot be observed with very good accuracy when the temperatures becomes too small. To overcome the difficulty of the convergence to a Dirac measure and to study more accurately the convergence to the equilibrium (as the behavior of the tail of the distribution function), we perform the following change of variable in velocity [19,27]

$$f(t,v) = \frac{1}{\sqrt{T(t)}}\tilde{f}(t,\xi), \quad \xi = v/\sqrt{T(t)},$$

where, without loss of generality, we assumed that the mean velocity of f is zero. Then, $\tilde{f}$ is solution to the following inelastic Boltzmann equation with a drift term

$$\frac{\partial \tilde{f}}{\partial t} - \frac{1-e^2}{4}\frac{\partial(\xi\tilde{f})}{\partial \xi} = Q(\tilde{f},\tilde{f}), \tag{32}$$

and T is given by Eq. (14).

Now, we have a system of two equations with unknowns $\tilde{f}$ and $T(t)$. Note that, in this simple Maxwellian case, the evolution of T is not directly coupled with the distribution function $\tilde{f}$ since $T(t)$ can be computed from (18). Up to a change of variables, we can always consider an initial data f_0 with mass equal to one, zero mean velocity and temperature equal to one. Then, the solution $\tilde{f}$ to (32) satisfies

$$\int_{\mathbb{R}} \tilde{f}(t,\xi)\begin{pmatrix}1\\ \xi\\ \xi^2\end{pmatrix} \mathrm{d}\xi = \begin{pmatrix}1\\ 0\\ 1\end{pmatrix}$$

and the equilibrium state is given by the Lorentz function [1]

$$\tilde{f}_\infty(\xi) = \frac{2}{\pi(1+\xi^2)^2}. \tag{33}$$

The approximation of the drift term in (32) is realized through fourth order centered differencies. The fourth order scheme has proved to be enough accurate in all the test cases here presented.

Note however that the equilibrium state is still quite difficult to approximate because of the slow zero convergence of the tails. Indeed, the third moment of $\tilde{f}$ is blowing-up at $t = +\infty$. To illustrate the slow convergence of the tail we present in Fig. 2 the evolution of the fourth moment with respect to the truncation of the distribution function $V = V_{\max}$ and to the number of Fourier modes N. We also present the evolution of the distribution function $\tilde{f}(t)$ in these new variables obtained with an uniform grid (256 points). As expected, the solution converges to (33) and the spectral method give the correct behavior of the tail even if it converges slowly to zero. Finally, in Fig. 3, we plot the numerical solution corresponding to initial data (i) and (ii), and observe the very good agreement (in log scale) between the numerical solution and the stationary Lorentz function (33).

In Fig. 4, we present a comparison between the long time behavior of the rescaled solution (in conventional variables) and the solution obtained with the non-rescaled method. It is evident how the Dirac delta is well captures by means of the scaling technique.

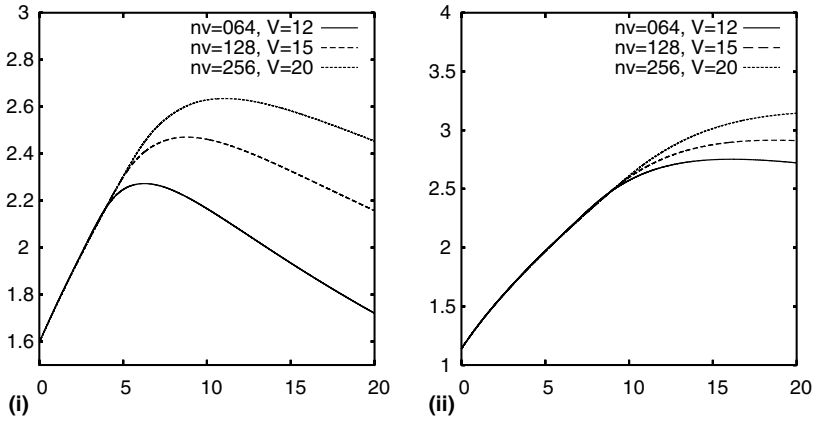

Fig. 2. 1D inelastic Maxwellian molecules: blow-up of the third order moment of the rescaled distribution $\tilde{f}$ corresponding to (i) and (ii).

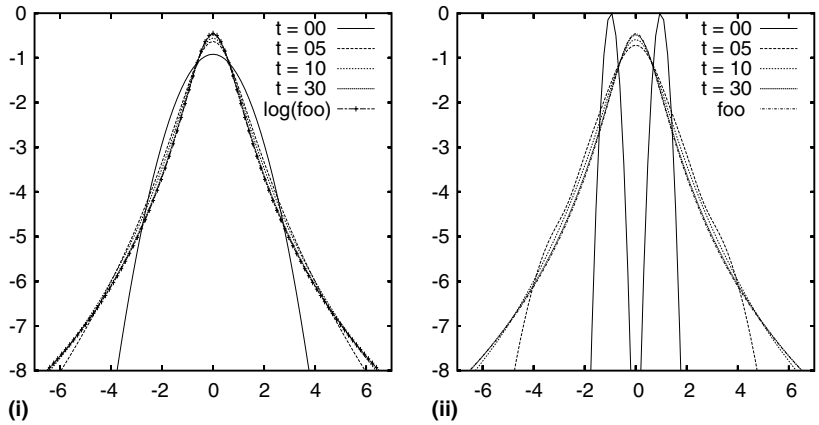

Fig. 3. 1D inelastic Maxwellian molecules: time evolution of the log-solution corresponding to initial data (i) and (ii) in rescaled variables.

4.1.2. The heated case

Now, we consider the heated granular gas case for Maxwell molecules in dimension one, so that we have a regularizing effect of the diffusive operator [37]

$$\frac{\partial f}{\partial t} - \varepsilon \Delta_v f = Q(f, f).$$

In this case, the Fourier transform in the one-dimensional case is known, which means that all moments are known analytically. For instance, the temperature does not converge to zero, and the relaxation of the temperature is given by

$$T(t) = (T_0 - T_\infty) \exp\left(-\frac{(1-e^2)}{2} t\right) + T_\infty,$$

where T_0 is the initial temperature and T_∞ is the expected temperature at time $t = +\infty$

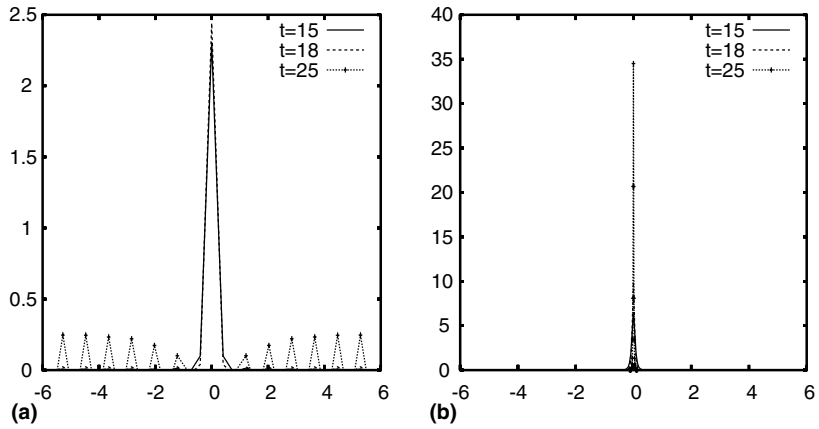

Fig. 4. 1D inelastic Maxwellian molecules: comparison of the large time solution corresponding to initial data (i) obtained from computations in classical variables (a) and from rescaled variables (b).

$$T_\infty = 4\varepsilon/(1-e^2).$$

Moreover the exact non-equilibrium steady-state solution was obtained in [10,34]. For this simple model, the high velocity tail is expected to behave as [5]

$$f_\infty(v) \sim \exp(-a|v|), \quad |v| \to \infty. \tag{34}$$

In Fig. 5, we present the evolution of the exact and numerical temperatures, which agree very well. Next in Fig. 6, we show the excellent agreement of the time evolution of the exact and numerical kurtosis of the distribution function computed in our case as

$$K(t) = \frac{M_4(t)}{T(t)},$$

where $M_4(t)$ is the fourth order moment of f.

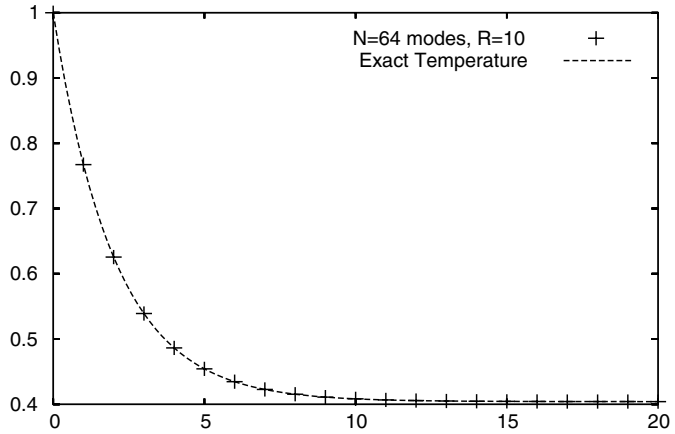

Fig. 5. 1D inelastic Maxwellian molecules with diffusion: time evolution of the temperature ($\varepsilon = 0.1$).

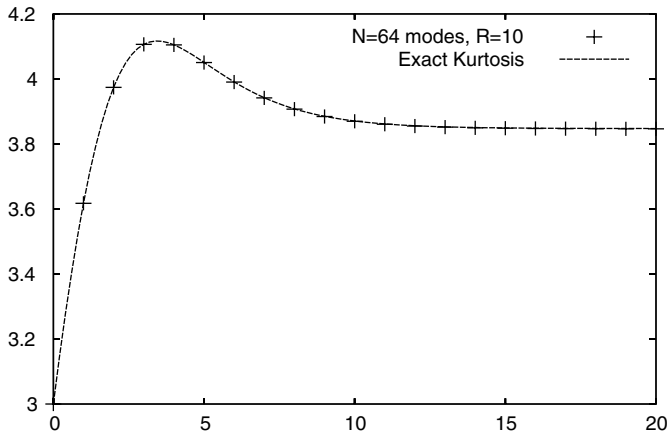

Fig. 6. 1D inelastic Maxwellian molecules with diffusion: time evolution of the kurtosis ($\varepsilon = 0.1$).

Due to the smoothness of the asymptotic state the rescaling technique is not necessary and the inelastic Boltzmann equation has been solved in direct variables.

Then, in Fig. 7, we plot stationary solutions obtained for different values of ε, the tail of $f(|v|)$ satisfies (34) for large velocities.

4.2. 1D model for hard-sphere molecules

This case is the most interesting from the physical viewpoint and the mathematical theory concerning the behavior of the temperature and the asymptotic states is not clearly established. However, some conjectures have been performed by physicists in the cooling case [21] and for driven systems [37]. The present method giving spectral accuracy on the collision operator seems to be particularly well suited to study numerically these problems.

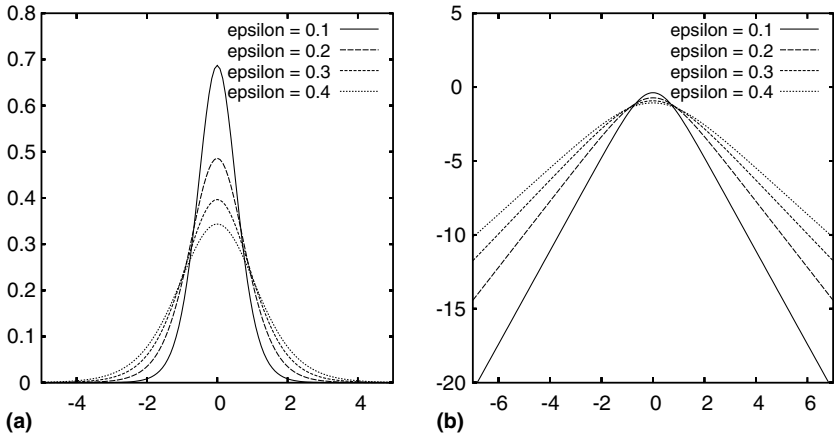

Fig. 7. 1D inelastic Maxwellian molecules with diffusion: time evolution of the solution for different values of ε.

4.2.1. Inelastic Boltzmann equation

As in the case of Maxwell molecules we perform computation in rescaled variables for the inelastic Boltzmann equation (32) to investigate the asymptotic state of the solution and the evolution of the temperature. In this case the evolution of $T(t)$ is not known exactly and has been obtained by solving numerically Eq. (14) for $\lambda = 1$.

We conjecture that the relaxation of the temperature can be written in the following form

$$T(t) = \frac{1}{(1 + a(t)t)^2},$$

where $a(t)$ converges to a constant which only depends on the restitution coefficient e. To numerically investigate the relaxation of the temperature, we first present the evolution of $T(t)$ for different initial data with the same initial temperature (see Fig. 8). Next, we plot the evolution of this quantity and its time derivative

$$\frac{1 - \sqrt{T(t)}}{t\sqrt{T(t)}},$$

which corresponds to $a(t)$ and $a'(t)$. As we expect $a(t)$ converges to a constant which only depend on the restitution coefficient e (assuming that $\rho = 1$, $u = 0$ and $T(0) = 1$) (see Fig. 9).

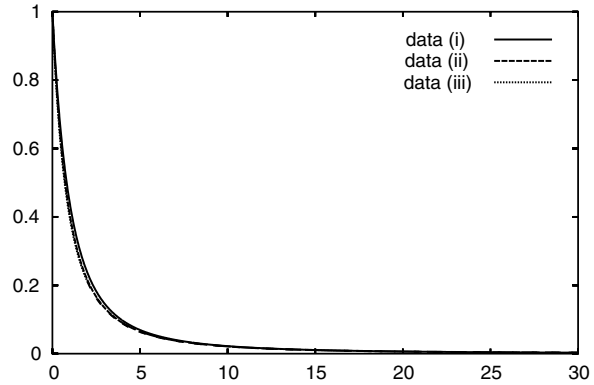

Fig. 8. 1D hard sphere molecules: time evolution of $T(t)$ corresponding to different initial data.

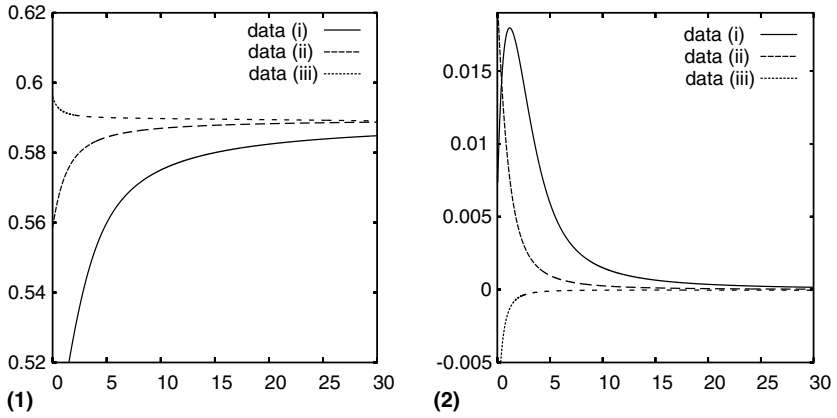

Fig. 9. 1D hard sphere molecules: time evolution of (1) $a(t)$ and (2) $a'(t)$ corresponding to the different initial data.

4.2.2. The heated case

Now, we consider the heated granular gas, so that we have the regularizing effect of the diffusive operator, but for hard sphere molecules

$$\frac{\partial f}{\partial t} - \varepsilon \Delta_v f = Q(f,f).$$

For this model, the evolution of the temperature is not known analytically, but the high velocity tail is expected to behave as [37]

$$f_\infty(v) \sim \exp(-a|v|^{3/2}), \quad |v| \to \infty. \tag{35}$$

Again no rescaling technique in this heated case has been used. On the one hand, we present the evolution of the temperature for a fixed initial datum and different values of ε (see Fig. 10). As expected the temperature is vanishing when ε goes to zero. On the other hand we plot in Fig. 11 stationary solutions

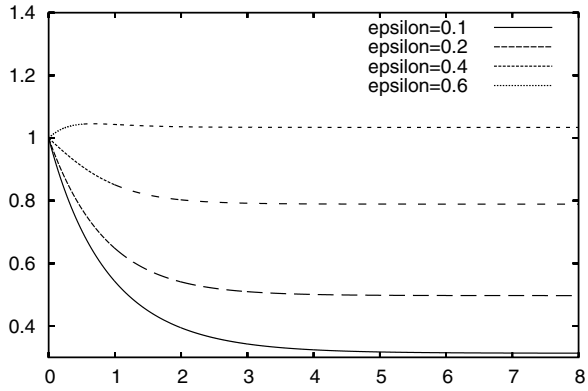

Fig. 10. 1D hard sphere molecules with diffusion: time evolution of $T(t)$ corresponding to different value of ε.

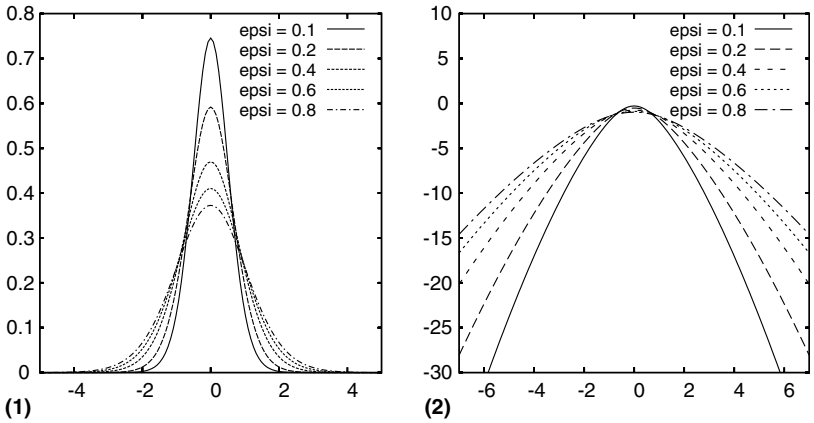

Fig. 11. 1D hard sphere molecules with diffusion: stationary distribution function (1) $f_\infty(v)$ and (2) $\log(f_\infty(v))$ corresponding to different initial data.

obtained for different values of ε, the tail of $f(|v|)$ satisfies (35) for large velocities. Moreover, the numerical results are accurate enough to evaluate the constant a in (35), which corresponds to the slope of the tail of the distribution function plotted in log scaled with respect to the diffusive coefficient ε.

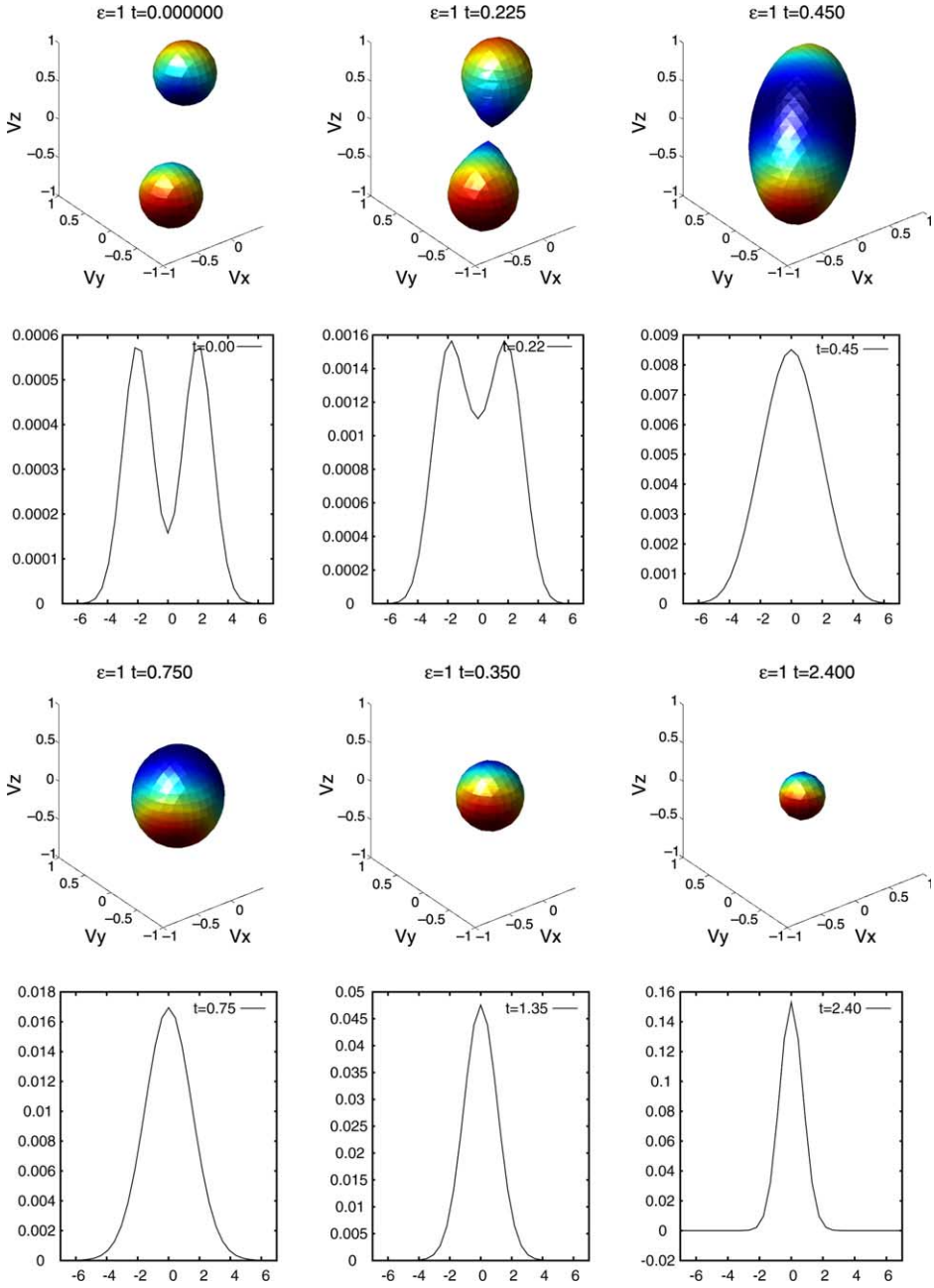

Fig. 12. 3D hard sphere molecules with diffusion: time evolution of isovalues $f(v, t) = c$ with $c = \max_v f(v, t)/3$ for $N = 32^3$.

4.3. 3D heated model for hard-sphere molecules

Asymptotic properties of stationary solutions for the uniformly heated 3D inelastic Boltzmann equation (1) have been recently discussed in several papers [5,13,24,37].

One of the most interesting question is the asymptotic behavior of the steady state distribution function f_∞

$$f_\infty = \lim_{t\to\infty} f(t,v),$$

for large $|v|$, where f is solution to

$$\frac{\partial f}{\partial t} - \varepsilon\Delta_v f = Q(f,f), \tag{36}$$

where

$$Q(f,f) = \frac{1}{4\pi}\int_{\mathbb{R}^3}\int_{S^2} |v-v_*|({}'f'f_*J - ff_*)\mathrm{d}n\,\mathrm{d}v_*,$$

with

$$J = \frac{1}{e^2}\frac{|{}'v - {}'v_*|}{|v-v_*|}.$$

It has been recently proven in [24] that the tail of the solution has a lower bound when t is large enough

$$f(t,v) \geqslant K\exp(-a|v|^{3/2}), \quad |v|\to\infty.$$

Later in [8], the authors has proved the corresponding upper bound and the tail of f behaves as in the one-dimensional case

$$f(t) \sim \exp(-a|v|^{3/2}), \quad |v|\to\infty, \tag{37}$$

where a depends on the quotient of the energy dissipation rate and the heat bath temperature. Moreover, the formal asymptotic has been shown in [37] for radially symmetric steady state.

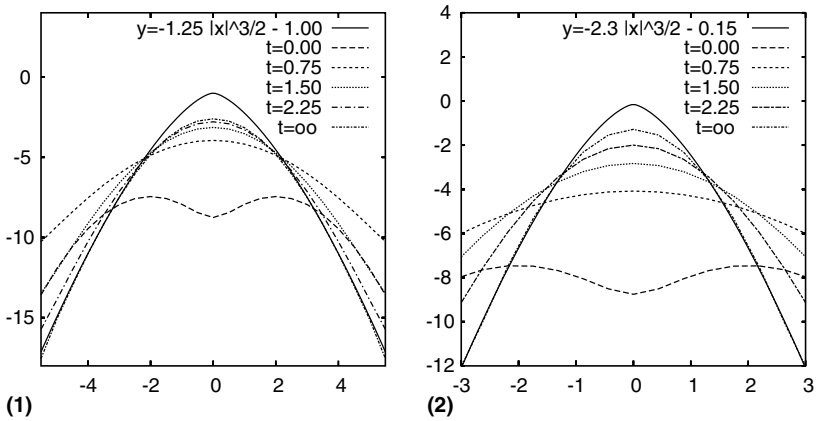

Fig. 13. 3D hard sphere molecules with diffusion: time evolution of $\log(f(t, v_x, v_y = 0, v_z = 0))$ for $\varepsilon = 0.5$ (*1*) and $\varepsilon = 0.1$ (*2*).

In Fig. 13, we consider an initial datum with zero mean velocity

$$f_0(v) = \frac{1}{2(2\pi)^{3/2}}\left(\exp(-|v-v_1|^2) + \exp(-|v+v_1|^2)\right), \quad v \in \mathbb{R}^3,$$

with $v_1 = (1.5, 1.5, 1.5)$. In Fig. 12, we plot the evolution of the isovalues of the distribution function in $3d$ when the diffusive coefficient is $\varepsilon = 1/10$. Next in Fig. 13, we report the corresponding slices of the distribution function in log scale in order to observe the behavior of the tail for large velocities for different values of $\epsilon = 1/10$ and $\varepsilon = 1/2$. Even with 32 modes in each direction, the tail of the distribution function is well approximated and can be compared in log scale with the expected behavior (37).

5. Conclusion

In this paper, we have presented an accurate deterministic method for the numerical approximation of the time dependent Boltzmann equation for granular gases. The method extends the Fourier spectral approximation for the collision operator already proposed for the classical Boltzmann operator [30,31]. Such a discretization is well suited for the accurate description of the distribution function evolution and gives an accurate approximation of steady states in $1D$ as well as in $3D$ in all the test cases in which exact solutions or exact theoretical results are available. This permits to test some interesting mathematical and physical conjectures.

Acknowledgement

Support by the European network HYKE, funded by the EC as contract HPRN-CT-2002-00282, is acknowledged.

References

[1] A. Baldassarri, U. Marini Bettolo Marconi, A. Puglisi, Kinetic models of inelastic gases, Mat. Mod. Meth. Appl. Sci. 12 (2002) 965–983.
[2] A. Baldassarri, U. Marini Bettolo Marconi, A. Puglisi, Cooling granular gases: the role of correlations in the velocity field, In Granular Gas Dynamics, Lecture Notes in Physics 624 (2003) 93–116.
[3] A.V. Bobylev, Exact solutions of the Boltzmann equation, Dokl. Akad. Nauk. USSR 225 (1975) 1296–1299 (in Russian).
[4] A.V. Bobylev, J.A. Carrillo, I.M. Gamba, On some properties of kinetic and hydrodynamics equations for inelastic interactions, J. Statist. Phys. 98 (2000) 743–773.
[5] A.V. Bobylev, C. Cercignani, Moment equations for a granular material in a thermal bath, J. Statist. Phys. 106 (2002) 547–567.
[6] A.V. Bobylev, C. Cercignani, Self-similar asymptotics for the Boltzmann equation with inelastic and elastic interactions, J. Statist. Phys. 110 (2003) 333–375.
[7] A.V. Bobylev, C. Cercignani, G. Toscani, Proof of an asymptotic property of self-similar solutions of the Boltzmann equation for granular materials, J. Statist. Phys. 111 (2003) 403–417.
[8] A.V. Bobylev, I.M. Gamba, V. Panferov, Moment inequalities and high energy tails for Boltzmann equations with inelastic interactions, J. Statist. Phys., in press.
[9] E. Ben-Naim, P.L. Krapivsky, The inelastic Maxwell model, In Granular Gas Dynamics, Lecture Notes in Physics 624 (2003) 63–92.
[10] N. Ben-Naim, P.L. Krapivski, Multiscaling in inelastic collisions, Phys. Rev. E 61 (2000) R5–R8.
[11] N.V. Brilliantov, T. Pöschel, Granular gases with impact-velocity dependend restitution coefficient, In Granular Gases, Lecture Notes in Physics 564 (2000) 100–124.
[12] C. Canuto, M.Y. Hussaini, A. Quarteroni, T.A. Zang, Spectral methods in fluid dynamics, Springer Verlag, New York, 1988.
[13] J.A. Carrillo, C. Cercignani, I.M. Gamba, Steady states of a Boltzmann equation for driven granular media, Phys. Rev. E 62 (2000) 7700–7707.

[14] C. Cercignani, Shear flow of a granular material, J. Statist. Phys. 102 (2001) 1407–1415.
[15] C. Cercignani, Recent developments in the mechanics of granular materialsFisica matematica e ingegneria delle strutture, Pitagora editrice, Bologna, 1995 pp. 119–132.
[16] C. Cercignani, R. Illner, M. Pulvirenti, The Mathematical Theory of Dilute Gases, Springer-Verlag, New York, 1995.
[17] P. Degond, L. Pareschi, G. Russo, Modeling and Computational Methods for Kinetic EquationsModeling and Simulation Science, Engineering and Technology, Birkhauser, Boston, 2004.
[18] M.H. Ernst, Exact solutions of the nonlinear Boltzmann equation and related kinetic models,Nonequilibrium Phenomena I. The Boltzmann equation, North-Holland, Amsterdam, 1983 pp. 52–119.
[19] M.H. Ernst, R. Brito, High energy tails for inelastic Maxwell models, Europhys. Lett. 43 (2002) 497–502.
[20] M.H. Ernst, R. Brito, Scaling solutions of inelastic Boltzmann equation with over-populated high energy tails, J. Statist. Phys. 109 (2002) 407–432.
[21] S.E. Esipov, T. Pöschel, The granular phase diagram, J. Stat. Phys. 86 (1997) 1385–1395.
[22] F. Filbet, G. Russo, High order numerical methods for the space non-homogeneous case for the Boltzmann equation, J. Comp. Phys. 176 (2003) 457–480.
[23] F. Filbet, G. Russo, A rescaling velocity method for kinetic equations, Work in progress.
[24] I.M. Gamba, V. Panferov, C. Villani, On the Boltzmann equation for diffusively excited granular media, Commun. Math. Phys., in press.
[25] I.M. Gamba, S. Rjasanow, R. Wagner, Direct simulation to the uniformly heated granular Boltzmann equation, Math. Comp. Model, in press.
[26] D. Gottlieb, S.A. Orszag, Numerical Analysis of Spectral Methods: Theory and Applications, SIAM CBMS-NSF Series, 1977.
[27] P.L. Krapivsky, E. Ben-Naim, Nontrivial velocity distributions in inelastic gases, J. Phys. A 35 (2002) LL147–LL152.
[28] G. Naldi, L. Pareschi, G. Toscani, Spectral methods for onedimensional kinetic models of granular flows and numerical quasi elastic limit, M2AN Math. Model. Numer. Anal. 37 (2003) 73–90.
[29] L. Pareschi, Computational methods and fast algorithms for Boltzmann equationsChapter 7, Lecture Notes on the discretization of the Boltzmann equation, World-Scientific, Singapore, 2003 pp. 527–548.
[30] L. Pareschi, B. Perthame, A Fourier spectral method for homogeneous Boltzmann equations, Trans. Theo. Stat. Phys. 25 (1996) 369–383.
[31] L. Pareschi, G. Russo, Numerical solution of the Boltzmann equation I: Spectrally accurate approximation of the collision operator, SIAM J. Numer. Anal. 37 (2000) 1217–1245.
[32] A. Pulvirenti, G. Toscani, Asymptotic properties of the inelastic Kac model, J. Statist. Phys. 114 (2004) 1453–1480.
[33] R. Ramírez, T. Pöschel, N.V. Brilliantov, T. Schwager, Coefficient of restitution of colliding viscoelastic spheres, Phys. Rev. E 60 (1999) 4465–4472.
[34] A. Santos, M.H. Ernst, Exact steady-state solution of the Boltzmann equation: a driven one-dimensional inelastic Maxwell gas, Phys. Rev. E 68 (2003).
[35] G. Toscani, Onedimensional kinetic models of granular flows, M2AN Math. Model. Numer. Anal. 34 (2000) 1277–1291.
[36] G. Toscani, Kinetic and hydrodinamic models of nearly elastic granular flows, Monatsch. Math. 142 (2004) 179–192.
[37] T.P.C. Van Noije, M.H. Ernst, Velocity distributions in homogeneous cooling and heated granular fluids, Gran. Matt. 1:57 (1998).